

The Heart Pacemaker by Cellular Automata on Complex Networks

Danuta Makowiec

Institute of Theoretical Physics and Astrophysics, Gdańsk University,
80-952 Gdańsk, ul.Wita Stwosza 57, Poland
fizdm@univ.gda.pl

Abstract. Specially desinged network of Greenberg-Hastings (GH) cellular automata is shown to be a reliable approximation to cardiac pacemaker. A complex network is built basing on a square lattice where some edges are rewired locally and with preference to link to cells which are more connected to other cells. GH automata are systems with cyclic intrinsic dynamics where three possible cell's states are characterized by timings — time steps spent in each state. Complex networks of GH automata evolve rhythmically with periods determined by timings. Diversity of oscillations coexisting in the system depends on network topology. Large variety in oscillations is interpreted as effectiveness to response to actual needs of a body.

Keywords: Greenberg-Hastings cellular automata, complex networks.

1 Introduction

The regular impulses, that result in rhythmic contractions of the heart, begin at the cardiac pacemaker called the sinoatrial node (SA node) [1]. The sinoatrial (SA) node is a piece of the cardiac tissue (3 mm wide and 7 mm long) located on the right atrium. The action potential originates in the SA node and then travels across the wall of the atrium to the atrioventricular (AV) node. In the same time the activity of the SA node spreads throughout the atria causing the atrial contraction. Then, the specialized conduction pathways: bundle of His and Purkinje fibers conduct the impulse throughout the ventricles causing the ventricle's contraction in an unison way.

Cellular automata have been used to model biological systems of different types, see, e.g., [2] for the review. In particular, cellular automata are known to model excitable media very well. The simplest cellular automata which are used to model the cardiac tissue are known as Greenberg-Hastings (GH) [3,4]. In order to include the heterogeneity of the real cardiac tissue, different cell connections between cellular automata have to be considered [5,6].

In the present work, following facts known from the SA node physiology, we propose a network which reconstructs the heterogeneity of the canine cardiac tissue, Section 2. Then we discuss properties of the GH cellular automaton in order to model activity of a SA nodal cell, Section 3. Finally, in Section 4, we

present results indicating that the specially constructed network of GH-type cellular automata leads to a reliable approximation of the cardiac pacemaker. The system evolves rhythmically with the period determined by intrinsic dynamics of the cellular automaton. Depending on the underlying network the diversity of oscillations varies. The large variety in oscillations we interpret as readiness of the system to the effective response to the actual needs of the body.

2 The Network Topology

For a long time the heart tissue was considered as syncytium - multi nucleated mass of cytoplasm that is not separated into individual cells [7]. Due to development of electron microscopy it became clear that cardiac cells — myocytes, were long and individual units, bounded on either end by intercalated discs. Then, it was shown that each disc was a gap which separated the opposed cell membranes. Each gap junction consists of many mechanisms which provide a pathway for direct cell-to-cell communication. Hence, in a simplified picture, one can see the cardiac tissue as a network consisting of branched chains of elongated cells which are connected by gap junctions — the only way to transmit the interactions.

There are known some network characteristics of cardiac tissue. It appears that a typical myocyte which builds the canine SA node has about 4.8 ± 0.7 nearest neighbors which are located as follows [8]: (a) about 0.7 ± 0.5 are side-to-side neighbors, (b) about 0.6 ± 0.7 are end-to-end neighbors, and (c) about 3.5 ± 1.9 are lateral neighbors. Hence about 74% connections are lateral. Moreover, it is known that side-to-side and lateral connections have relatively small gap junctions, and therefore, their efficiency in transmitting signals is considered as less effective than in the case of the end-to-end connections.

To replicate the nodal properties let us consider a square lattice and introduce preferences to askew connections in the following way:

(I) For a given probability d , a vertical or horizontal link is created with $d/2$ probability while any askew edge is created with $2 * d$ probability.

It is easy to check that the canine SA network is about to be restored if we work with $d = 0.45$, see Fig. 2. The cells from the leftmost column and rightmost column form the interface to crista terminalis cells — cardiac tissue which conducts signals from the SA node to the AV node. Therefore, we additionally link them via horizontal connections. Moreover, we connect unlinked cells to their nearest right cells. By these two extra rules, some additional horizontal connections are added. Finally, in case of $d = 0.45$, a resulting network has about 10% vertical, 11% horizontal and 79% askew connections.

The introduced structure is flat. To make the surface uneven we propose the local rewiring procedure which additionally sets the preference to the connectivity between a cell and the network. The rewiring algorithm consists of the following rules: see Fig. 2: let p is *probability of rewiring* then

(II) for a given cell A a less connected cell is unlinked. The probability to unlink a B cell from a vertex A is calculated as: $p_{unlink} = \frac{p}{\deg(B)}$, where $\deg(B)$ is degree of a vertex B . The rewiring is local what means that a new cell B' which

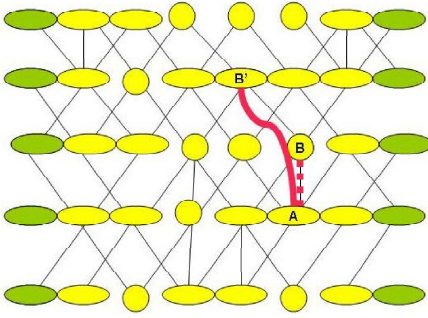


Fig. 1. Construction of a network: most of connections are diagonal because of (I) rule; the leftmost and rightmost cells of each row (input to crista terminalis) are connected end-to-end with their neighbors; red lines illustrate the rewiring rule (II). Color on-line.

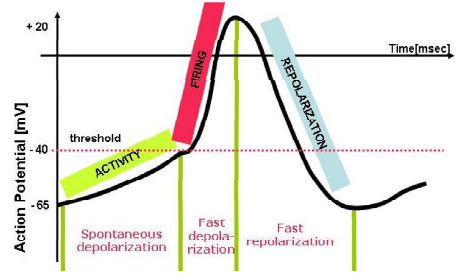


Fig. 2. Changes in the electrical potential on the membrane of a typical cell from the SA node, adapted from [1], color on-line

will be linked to the cell *A* is chosen from actual neighbors of *B* automaton. To preserve the line structure, any horizontal connection is forbidden to be rewired. Unlinking from a leaf is forbidden also.

In Fig.3 left we show vertex degree distributions in networks resulted after applying the above algorithm to each edge with $p = 0.01$ and repeating the procedure 0, 100 and 500 Monte Carlo steps (MCS). It appears that due to locality in rewiring, the network is only slightly modified. In Fig.3 right a typical example of connections is shown. A network is almost flat and slightly heterogeneous — there are several vertices with the vertex degree larger two times than the average vertex degree.

3 The FRA Cellular Automaton

In the simplified picture, there are three main stages in a cell dynamics which we will call *firing*, *repoliarization* and *activity* as it is indicated in Fig. 2. Being in the firing state a cell initiates the action potential in the neighboring cells. But to read the signal from a neighbor, the cell has to be in the activity state. If the cell is in the repolarization state then there is no way neither to be excited nor to excite the other cell. If a cell does not receive a stimulus from a neighbor, then after some time the cell starts firing because of its intrinsic cycle dynamics.

The above description suggests considering a cellular automaton as a three-state automaton F, R, A which performs intrinsic cyclic evolution $F \rightarrow R \rightarrow A \rightarrow F \rightarrow \dots$. Let us assume that there are fixed numbers of steps n_F, n_R, n_A during which each automaton stays in corresponding states. This proposition is related to the original GH cellular automata [3]. Our modifications follow considerations of Bub *et.al* [9] — we skip constraints for self-excitation of a cell. Here, each automaton after spending n_A steps in *A* state changes its state to *F*.

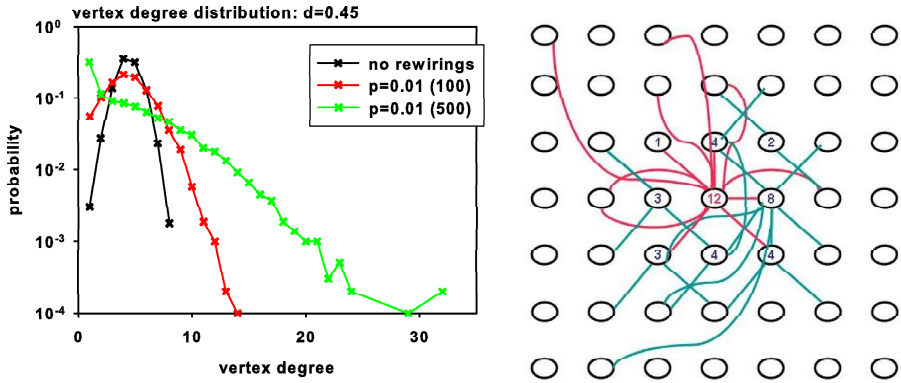


Fig. 3. Left figure: the vertex distribution in the networks considered. Right figure: a piece of a typical connections. Neighbors of a vertex with high degree are presented - red lines; green lines describe links of Moore neighbors of the vertex. Numbers are degrees of vertices. Color on-line.

The introduced intrinsic dynamic rule is deterministic what is closely related with the physiologically observed fact that the lengths of the fast depolarization and repolarization are strongly fixed. Hence any changes in timings n_F, n_R and n_A from a period to a period should be rather limited. Therefore, let us consider the little probable possibility of shortening each of n_F, n_R and n_A value. It effects in that there is a nonzero probability for a switch of the actual automaton state to the next state in its intrinsic cycle. Formally, we propose that cellular automaton performs the stochastic evolution governed by the following rule:

$$\begin{pmatrix} \sigma \\ s \end{pmatrix} (t) \xrightarrow{t \rightarrow t+1} \begin{cases} \begin{pmatrix} next(\sigma) \\ 1 \end{pmatrix} & \text{with probability } \left(\frac{s}{n_S}\right)^\xi \\ \begin{pmatrix} \sigma \\ s+1 \end{pmatrix} & \text{with probability } 1 - \left(\frac{s}{n_S}\right)^\xi \end{cases} \quad (1)$$

where σ is any of F, R, A states, s counts the number of steps which an automaton actually stays in a σ state and $next$ means the subsequent state in the intrinsic cell cycle. If $\xi \gg 1$ then we restore the deterministic evolution. Notice that for $\xi > 1$ only very few last steps could be skipped and therefore the effective timings are closely determined by values of n_F, n_R and n_A .

Finally, let us assume that the threshold for firing an automaton by its nearest neighbors equals to 1, i.e., at least two neighbors in the *firing* state are needed to switch an automaton from the state of *activity* to the *firing* state. However, since the horizontal connections are known to be more efficient than others, we additionally assume that the influence of the horizontal connections is doubled — only one left or right neighbor being in the *firing* state is able to activate the cell. We will refer to described cellular automata as *FRA-CA*.

4 Results

Our earlier studies of FRA-CA have provided that in case of the two FRA-CA evolving according to the deterministic version of 1, only the three stable solutions are possible, [10,11]:

- *the rules adjusted evolution*: if the result of both rules: intrinsic and interactions between the automata, is the same;
- *the alternating impacts evolution*: if within each period two events of impacts take place. The first event means **A** automaton is impacted by **B** automaton — **A** automaton is switched to *firing*. Then the second event occurs — **B** automaton is impacted by **A** automaton what switches **B** automaton to *firing*.
- *the quiet evolution*: there are not any impacts between the automata.

One can say that the alternating impacts evolution is the maximally active dynamics since both cells of a pair intensively interact with each other. Because of the intensity of impacts the intrinsic periods of both automata are shortened to the shortest period possible $T^* = n_F + n_R + 1$. The other two evolutions are also periodic but the period is equal to the intrinsic period of the FRA-CA, i.e., $T = n_F + n_R + n_A$.

Moreover, it has appeared that in case of a line of many FRA-CA with open boundary, the system always reaches the periodic state and only one of the two periods happens — either T or T^* . Depending on the model parameters the probability to find which period occur is different. If $n_F \leq n_R$ then the solution with the period T happens. If $n_F > n_R$ then the solution with the period T^* is significantly more probable. It also has been found that if $n_R > n_F$ then all automata from a line follow the rules adjusted evolution. Case of $n_R > n_F$ is physiologically important because it is known that the time used by a myocyte for the fast depolarization is shorter than the time spent on repolarization processes or during the slow depolarization [12].

At present we ask whether stationary evolution of FRA-CA distributed on networks described in Section 2 with dynamics (1) is periodic. The network state is evaluated by number of FRA-CA staying in the *firing* state in the leftmost column I_{left} and in the rightmost column I_{right} . These currents are assumed to imitate signals which arrive to outputs — the crista terminalis. Additionally, we also consider a total signal I_{total} which counts all cells which are in *firing* state.

To identify oscillations in the signal we calculate the power spectrum $S(f)$ of signals by the Fast Fourier Transform. In Fig.4 we show representative signals obtained for various model parameters from networks consisting of $N = 10\,000$ FRA-CA. It appears that oscillations of the total signal I_{total} are rather weak. But the signals from the borders of the networks I_{left} and I_{right} are noticeable periodic. There are evident maxima in all plots of power spectra. These maxima are located close to $1/T^*$ and $1/T$. They are moved a little to the right and wide because of the stochasticity of the intrinsic dynamics.

Let us assume that a given frequency f is present in a signal if its power spectrum $S(f)$ value is greater than 10^{-7} . In Fig. 5 we present all frequencies extracted in this way from the spectra of I_{total} , I_{left} and I_{right} when $n_F = 10$, $n_A = 20$ and for different values of n_R . The results are collected according to

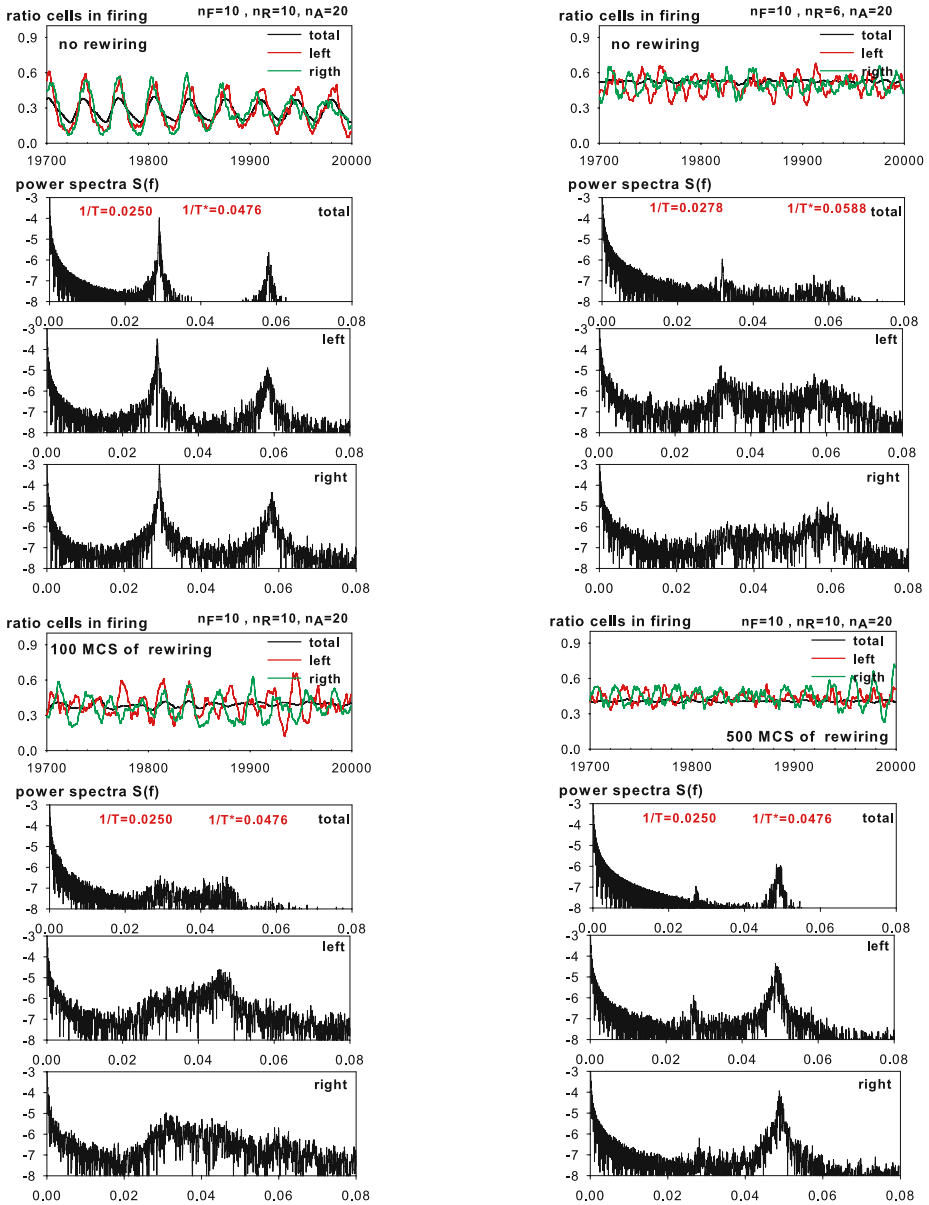


Fig. 4. Typical time series of the output signals I_{total} , I_{left} and I_{right} and their power spectra (log plots) for different networks. Timings are given above the plots of time series. Color on-line.

the three types of network settings: no rewiring, 100 MCS of rewiring and 500 MCS of rewiring.

It appears that in case of non rewired lattice the system oscillates with one dominant period. For n_R significantly smaller than n_F (here $n_R < 6$) the period

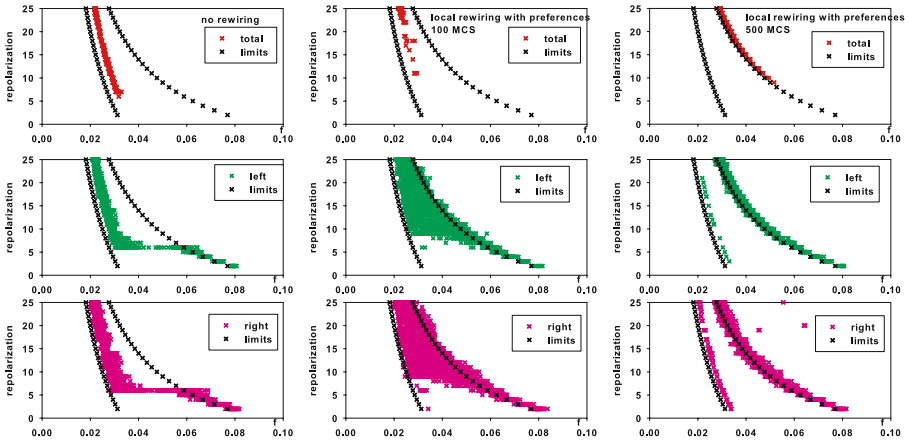


Fig. 5. Dominant frequencies identified in the output signals I_{total} , I_{left} and I_{right} in different networks. Black points correspond to $1/T$ and $1/T^*$ frequencies. Color on-line.

is about T^* . But then the evolution switches to oscillations with the period T what indicates that most of FRA-CA is not influenced by neighbors and rather follow the intrinsic cyclic dynamics. This observation does not hold if the network is modified by rewiring. In case of a little modification (100 MCS) for any n_R the active oscillations with T^* period are always present. Moreover, the same time the wide spectrum of possible oscillations between the T^* and T periods is present in the system. Hence the interactions among cells vividly influence the system evolution. Finally, if the network is strongly modified (case of 500 MCS) then only two basic oscillations T and T^* are present and T^* is dominant.

5 Conclusions

In the following by simulations we have investigated influence of topology of a network to oscillations of multi FRA-CA systems. We have found that all systems considered evolve rhythmically with the periods determined by the cell's intrinsic dynamics. However, in case of the heterogeneous network more oscillations coexists together. Moreover there is not present the transition in the dominant oscillation when timings are changed. Therefore the FRA-CA on the heterogeneous networks seem to better reconstruct properties of the real pacemaker — such systems can answer more flexible to external regulating systems.

The simulations were performed with 10 000 FRA-CA. In case of humans it is known that the SA node consists of about 70 000 cells[1]. Hence to obtain on-to-one mapping we should increase the size of simulated systems. Moreover, it is known that the SA nodal cells are not identical. Fortunately, the differences between cells are systematic — the further from the center of the sinus node the cell is located, then the difference between a center cell and a periphery

cell is more evident. Therefore the work on enlarging the system, should also incorporate the fact of the cell diversity.

The presented investigations are only preliminary and are not claimed to be completed. However, we hope that by comparing the physiologically known properties and our results we provide hints on the cellular network of the SA node.

Acknowledgment. Author thanks to University of Gdańsk for support: BW-5400-5-0090-08.

References

1. Klabunde, R.E.: Cardiovascular Physiology Concepts, <http://www.cvphysiology.com>
2. Ermentrout, G.B., Edelstein-Keshet, L.: Cellular Automata Approaches to Biological Modeling. *J. Theor. Biol.* 160, 97–133 (1993)
3. Greenberg, J.M., Hastings, S.P.: Spatial Patterns for Discrete Models of Diffusion in Excitable Media. *SIAM J. Appl. Math.* 34, 515–523 (1978)
4. Greenberg, J.M., Greene, C., Hastings, S.P.: Remarks on a 25 Year Old Theorem on Two-dimensional Cellular Automata. *Int. J. Unconv. Comp.* 1, 399–402 (2005)
5. Markus, M., Hess, B.: Isotropic Cellular Automaton for Modeling Excitatory Media. *Nature* 347, 56–58 (1990)
6. Bub, G., Shrier, A., Glass, L.: Spiral Wave Generation in Heterogeneous Excitable Media. *Phys.Rev.Lett.* 88, 058101–1–4 (2002)
7. Saffitz, J.E., Lerner, D.L., Yamada, K.A.: Gap Junctions Distribution and Regulation in the Heart. In: Zipes, D.P., Jalife, J. (eds.) *Cardiac Electrophysiology. From Cell to Bedside*, pp. 181–191. Saunders Co., Philadelphia (2004)
8. Luke, R.A., Saffitz, J.E.: Remodeling of Ventricular Conduction Pathways in Healed Canine Infarct Border Zones. *J. Clin. Invest.* 87(5), 1594–1602 (1991)
9. Bub, G., Shrier, A., Glass, L.: Global Organization of Dynamics in Oscillatory Heterogeneous Excitable Media. *Phys. Rev. Lett.* 94, 028105–1–4 (2005)
10. Makowiec, D.: On Cellular Automata Modeling of Cardiac Pacemaker. *Journal of Cellular Automata* (to appear, 2008)
11. Makowiec, D.: Cellular Automata Model of Cardiac Pacemaker. *Acta Phys. Pol. B* (to appear, 2008)
12. Kodama, I., Honjo, H., Boyett, M.R.: Are We Lost in the Labyrinth of the Sinoatrial Node Pacemaker Mechanism? *Journal of Cardiovascular Electrophysiology* 13(12), 1303–1305 (2002)